Whole-genome doubling promotes immune evasion in TNBC by epigenetically silencing of antigen presentation pathways

P. Foidart[1,2,3], Z. Li[1,2,3], X. Cai[1,2,3], M. Seehawer[1,2,3], D. D. Brown[6], A. Tawawalla[1], P. Baldominos[4,5], S. Parvin[1,2,3], J. Nishida[1,2,3], E. Rojas-Jimenez[1,2,3], T. M. Bui[1,2,3], B. Diciaccio[1,2,3], R. Kumar[7,8], B. T. Schlegel[7,8], M-A. Goyette[1,2,3], T-J. Scales[11], P. Yan[1,2,3], X. Qiu[9], R. Li[9], Y. Jiang[9], Y. Xie[9], X-Y. Huang[1], L. E. Stevens[1,2,3], P. Cejas[9], L. Mangiante[10], C. I. Sotomayor Vivas[10], K. E. Houlahan[10], C. Curtis[10], S. Oesterreich[7,8], I. S. Harris[11], A. G. Letai[1,2,3], A. V. Lee[6,7,8], H. W. Long[9], J. Agudo[4,5], K. Polyak[1,2,3]

[1]Department of Medical Oncology, Dana-Farber Cancer Institute (DFCI), Boston, USA. [2]Department of Medicine, Brigham and Women's Hospital, Boston, USA [3]Department of Medicine, Harvard Medical School, Boston, USA. [4]Department of Cancer Immunology and Virology, DFCI, Boston, USA. [5]Department of Immunology, Harvard Medical School, Boston, USA. [6]Institute for Precision Medicine, University of Pittsburgh, Pittsburgh, USA. [7]Women's Cancer Research Center, UPMC Hillman Cancer Center, Magee-Women's Research Institute, Pittsburgh, USA. [8]Department of Pharmacology and Chemical Biology, University of Pittsburgh, Pittsburgh, USA. [9]Center for Functional Cancer Epigenetics, DFCI, Boston, USA. [0]Stanford Cancer Institute, Stanford University School of Medicine, Stanford, USA., [11]University of Rochester Medical Center, Rochester, USA.

Introduction

Triple-negative breast cancer (TNBC) accounts for 10-15% of all breast cancers. The combination of chemotherapy and immunotherapy (ICI: immune checkpoint inhibitor) is now a standard in stages II-III TNBC. In advanced TNBC, this regimen is only in a subset of tumors presenting a high expression of PD-L1.

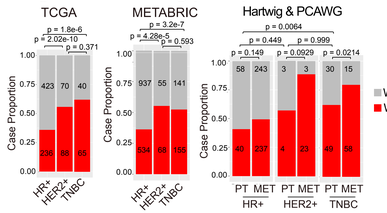
However, recent data indicate that tumors having a whole genome doubling (WGD) are more sensitive to ICI. Almost all human cells are diploid. Nevertheless, a WGD happens when regulation system maintaining the diploid status fail. The WGD+ cells are polyploid, oncogenic and facilitate tumorigenesis. The WGD occurs in 44% of breast cancers and has been correlated to advanced cases, lower survival and higher resistance to chemotherapies and targeted therapies. Therefore, WGD might play an important role towards immune escape and sensitization to ICI.

We demonstrate that WGD promoted immune evasion by enabling escape from CD8⁺ T cell-mediated immune responses, rendering WGD+ tumors more sensitive to anti-PD-L1 therapy. Moreover WGD+ cancer cells exhibit impaired antigen presentation, driven in part by a reduced response to IFN-γ and epigenetic silencing of MHC class I transcriptional regulators.

Funding-landed

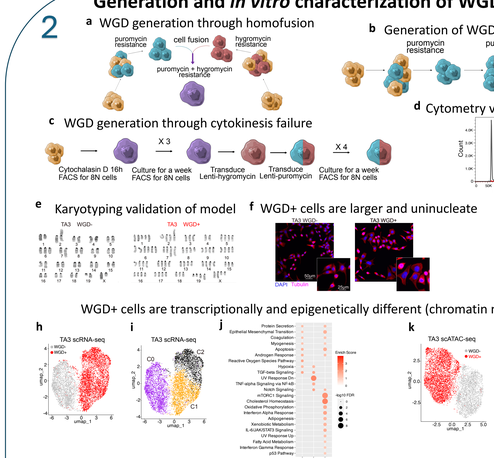
Funding-candidate

1 Whole genome doubling (WGD) is more prevalent in TNBC



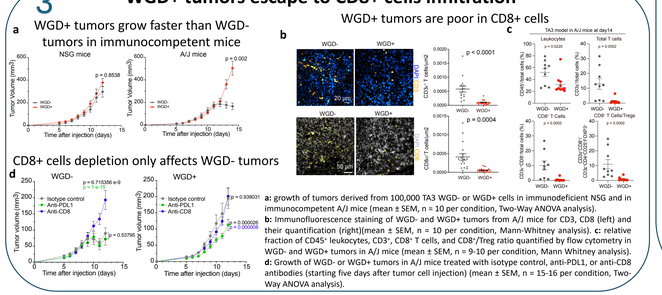
Calling WGD from DNA in three breast cancers databases using the Absolute Algorithm

2 Generation and *in vitro* characterization of WGD+ cells



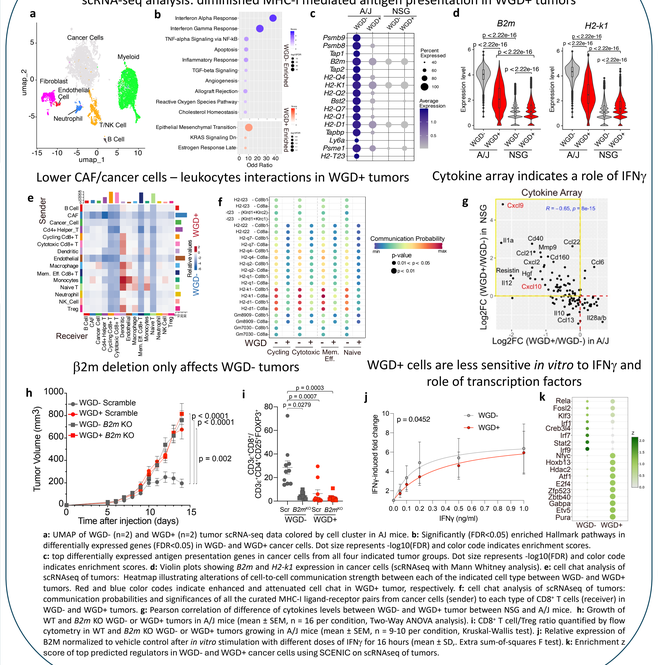
a-b: Parental cells were transfected with vectors conferring a resistance either to puromycin or hygromycin before an homofusion of cells containing the two different plasmid using a polyethyleneglycol-induced fusion of membranes (a) or a subsequent transfection with the other plasmid of resistance (b). Selection of cells was done by double antibiotic therapy. **c:** Obtention of WGD cells was also performed after cytochalasin D treatment and cytometry sorting of cells being 8n in G2/S phase of cell cycle. **d-e:** Confirmation of WGD obtention by flow cytometry through Hoechst staining (d) and karyotyping (e). **f:** Immunofluorescence staining of TA3 Hauschka (TA3) WGD- and WGD+ cells with anti-tubulin antibody and DAPI. **g:** *In vitro*, no difference of proliferation was observed between WGD- and WGD+ cells in basal conditions. **h-j:** UMAP of scRNA-seq of TA3 WGD- and WGD+ cells colored by genotype (h) and cell clusters (i) and enrichment of hallmark pathways in the marker genes of three subclusters in panel i (j). **k-l:** UMAP of scATAC-seq of TA3 WGD- and WGD+ cells colored by genotype (k) and the fragments counts of both genotypes (l).

3 WGD+ tumors escape to CD8+ cells infiltration



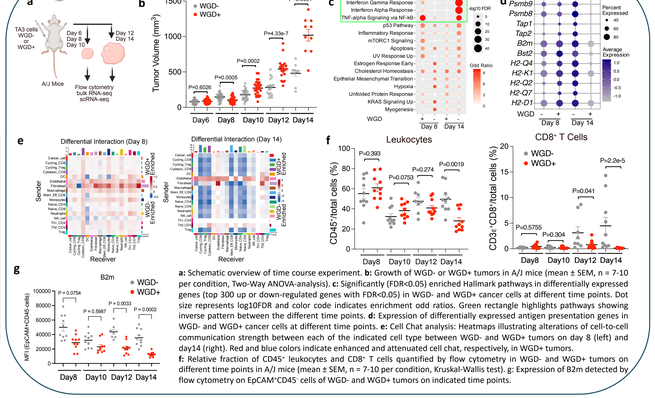
a: growth of tumors derived from 100,000 TA3 WGD- or WGD+ cells in immunodeficient NSG and in immunocompetent A/J mice (mean ± SEM, n = 10 per condition, Two-Way ANOVA analysis).
b: Immunofluorescence staining of WGD- and WGD+ tumors from A/J mice for CD3, CD8 (left) and their quantification (right)(mean ± SEM, n = 10 per condition, Mann-Whitney analysis). **c:** relative fraction of CD45⁺ leukocytes, CD3⁺, CD8⁺ T cells, and CD8⁺/Treg ratio quantified by flow cytometry in WGD- and WGD+ tumors in A/J mice (mean ± SEM, n = 9-10 per condition, Mann Whitney analysis).
d: Growth of WGD- or WGD+ tumors in A/J mice treated with isotype control, anti-PDL1, or anti-CD8 antibodies (starting five days after tumor cell injection) (mean ± SEM, n = 15-16 per condition, Two-Way ANOVA analysis).

4 Antigen presentation is reduced in WGD+ tumors by lower sensitivity to IFNγ



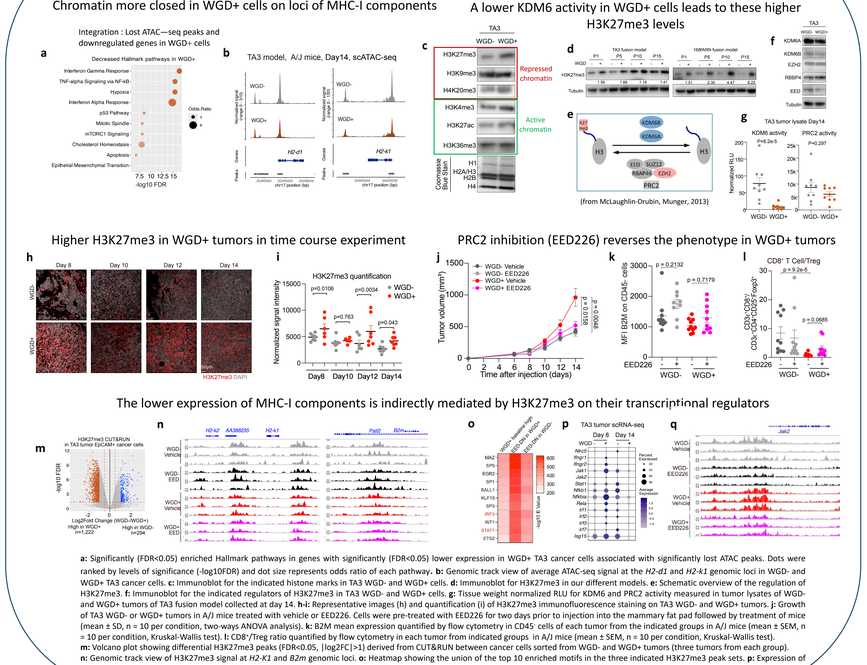
a: UMAP of WGD- (n=2) and WGD+ (n=2) tumor scRNA-seq data colored by cell cluster in AJ mice. **b:** Significantly (FDR<0.05) enriched Hallmark pathways in differentially expressed genes (FDR<0.05) in WGD- and WGD+ cancer cells. Dot size represents -log10(FDR) and color code indicates enrichment scores. **c:** top differentially expressed antigen presentation genes in cancer cells from all four indicated tumor groups. Dot size represents -log10(FDR) and color code indicates enrichment scores. **d:** Violin plots showing *B2m* and *H2-K1* expression in cancer cells (scRNAseq with Mann Whitney analysis). **e:** cell chat analysis of scRNAseq of tumors: Heatmap illustrating alterations of cell-to-cell communication strength between each of the indicated cell type between WGD- and WGD+ tumors. Red and blue color codes indicate enhanced and attenuated cell chat in WGD+ tumor, respectively. **f:** cell chat analysis of scRNAseq of tumors: communication probabilities and significances of all the curated MHC-I ligand-receptor pairs from cancer cells (sender) to each type of CD8⁺ T cells (receiver) in WGD- and WGD+ tumors. **g:** Pearson correlation of difference of cytokines levels between WGD- and WGD+ tumor between NSG and A/J mice. **h:** Growth of WT and *B2m* KO WGD- or WGD+ tumors in A/J mice (mean ± SEM, n = 16 per condition, Two-Way ANOVA analysis). **i:** CD8⁺ T cell/Treg ratio quantified by flow cytometry in WT and *B2m* KO WGD- or WGD+ tumors growing in A/J mice (mean ± SEM, n = 9-10 per condition, Kruskal-Wallis test). **j:** Relative expression of B2M normalized to vehicle control after *in vitro* stimulation with different doses of IFNγ for 16 hours (mean ± SD,. Extra sum-of-squares F test). **k:** Enrichment z score of top predicted regulators in WGD- and WGD+ cancer cells using SCENIC on scRNAseq of tumors.

5 Time-course :WGD+ tumors are initially more immunogenic

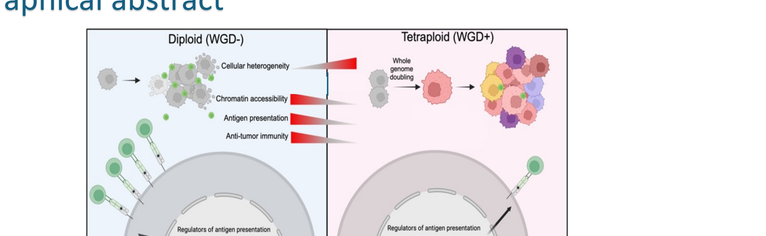


a: Schematic overview of time course experiment. **b:** Growth of WGD- or WGD+ tumors in A/J mice (mean ± SEM, n = 7-10 per condition, Two-Way ANOVA analysis). **c:** Significantly (FDR<0.05) enriched Hallmark pathways in differentially expressed genes (top 300 up or down-regulated genes with FDR<0.05) in WGD- and WGD+ cancer cells at different time points. Dot size represents log10FDR and color code indicates enrichment odd ratios. Green rectangle highlights pathways showing inverse pattern between the different time points. **d:** Expression of differentially expressed antigen presentation genes in WGD- and WGD+ cancer cells at different time points. **e:** Cell Chat analysis: Heatmaps illustrating alterations of cell-to-cell communication strength between each of the indicated cell type between WGD- and WGD+ tumors on day 8 (left) and day14 (right). Red and blue colors indicate enhanced and attenuated cell chat, respectively, in WGD+ tumors.
f: Relative fraction of CD45⁺ leukocytes and CD8⁺ T cells quantified by flow cytometry in WGD- and WGD+ tumors on different time points in A/J mice (mean ± SEM, n = 7-10 per condition, Kruskal-Wallis test). **g:** Expression of B2m detected by flow cytometry on EpCAM⁺CD45⁻ cells of WGD- and WGD+ tumors on indicated time points.

6 WGD drives immune evasion via histone H3K27me3 epigenetic silencing of antigen presentation pathways



The lower expression of MHC-I components is indirectly mediated by H3K27me3 on their transcriptional regulators



a: Significantly (FDR<0.05) enriched Hallmark pathways in genes with significantly (FDR<0.05) lower expression in WGD+ TA3 cancer cells associated with significantly lost ATAC peaks. Dots were ranked by levels of significance (-log10FDR) and dot size represents odds ratio of each pathway. **b:** Genomic track view of average ATAC-seq signal at the *H2-d1* and *H2-k1* genomic loci in WGD- and WGD+ TA3 cancer cells. **c:** Immunoblot for the indicated histone marks in TA3 WGD- and WGD+ cells. **d:** Immunoblot for H3K27me3. **e:** Schematic overview of the regulation of H3K27me3. **f:** Immunoblot for the indicated regulators of H3K27me3 in TA3 WGD- and WGD+ cells. **g:** Tissue weight normalized RLU for KDM6 and PRC2 activity measured in tumor lysates of WGD- and WGD+ tumors of TA3 fusion model collected at day 14. **h-i:** Representative images (h) and quantification (i) of H3K27me3 immunofluorescence staining on TA3 WGD- and WGD+ tumors. **j:** Growth of TA3 WGD- or WGD+ tumors in A/J mice treated with vehicle or EED226. Cells were pre-treated with EED226 for two days prior to injection into the mammary fat pad followed by treatment of mice (mean ± SD, n = 10 per condition, two-ways ANOVA analysis). **k:** B2M mean expression quantified by flow cytometry in CD45⁻ cells of each tumor from the indicated groups in A/J mice (mean ± SEM, n = 10 per condition, Kruskal-Wallis test). **l:** CD8⁺/Treg ratio quantified by flow cytometry in each tumor from indicated groups in A/J mice (mean ± SEM, n = 10 per condition, Kruskal-Wallis test).
m: Volcano plot showing differential H3K27me3 peaks (FDR<0.05, |log2FC|>1) derived from CUT&RUN between cancer cells sorted from WGD- and WGD+ tumors (three tumors from each group).
n: Genomic track view of H3K27me3 signal at *H2-K1* and *B2m* genomic loci. **o:** Heatmap showing the union of the top 10 enriched motifs in the three indicated H3K27me3 peak sets. **p:** Expression of genes encoding interferon response regulators in WGD- or WGD+ cancer cells from the time course experiment. **q:** Genomic track view of H3K27me3 signal at *Jak2* genomic loci.

Graphical abstract

SAN ANTONIO BREAST CANCER SYMPOSIUM®

UT Health San Antonio Mays Cancer Center

AACR American Association for Cancer Research

Pierre Foidart
MD PhD (medical oncologist)
CHU Liège ...